Two-step Broadband Equivalent Circuit Modeling Method for Power Transformer Winding Based on Frequency Response Analysis and Bayesian Optimization

Yu Chen, Jiangnan Liu, Yuxuan Ding*, Yaping Du, Binghao Li, Chenguo Yao, Zhongyong Zhao**

Email: yu2000.chen@connect.polyu.hk

The Hong Kong Polytechnic University (PolyU)

Early access in IEEE TDEI

Paper code:

More about me:

Introduction

Power transformers are vital components in power systems, ensuring reliable transmission, conversion, and voltage regulation. Winding deformation, often caused by short-circuit currents, accounts for nearly 30% of transformer faults. Detecting such faults efficiently is critical for system stability and economic operation. Among diagnostic techniques, Frequency Response Analysis (FRA) has become the most widely adopted due to its precision, non-destructive nature, and cost-effectiveness.

Accurate modeling of transformer windings is essential to interpret FRA fingerprints and simulate fault scenarios. Equivalent circuit models allow cost-free simulations, reducing reliance on destructive experiments and expert judgment. However, building a broadband equivalent circuit with physical significance remains challenging, limiting both fault mechanism understanding and data generation for data-driven diagnosis.

Existing modeling approaches face limitations:

1. Black-box models reproduce FRA fingerprints but lack physical meaning.
2. White-box models are accurate but computationally expensive and deviate from measured data.
3. Grey-box models combine physical knowledge with optimization but require parameter tuning.

Thus, there is a need for a generalizable, efficient, and physically meaningful modeling method that bridges the gap between accuracy and computational feasibility.

Methodology

Principle of FRA

- Under high-frequency excitation (1–1000 kHz), the transformer core influence is negligible.
- The winding is modeled as a passive two-port network with distributed parameters (R, L, C, G).
- Winding deformation alters these parameters, shifting resonance points and changing the FRA fingerprint.

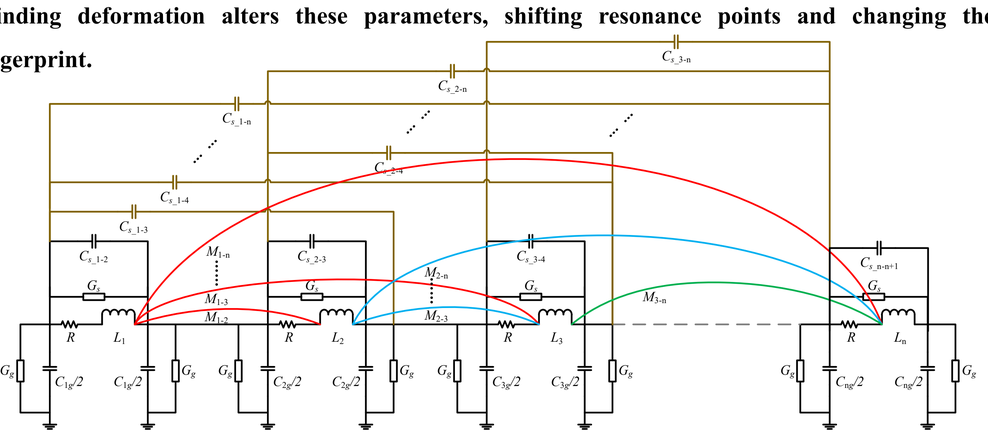

Figure 1: The proposed equivalent circuit model of transformer winding, considering long-distance mutual inductances and capacitances.

- ✓ A ladder network model is adopted, representing the winding as cascaded units.
- ✓ Each unit includes resistance (copper loss), self- and mutual inductances, inter-disk capacitances, ground capacitances, and leakage conductances.
- ✓ Long-distance mutual inductances and capacitances are incorporated to improve high-frequency accuracy.

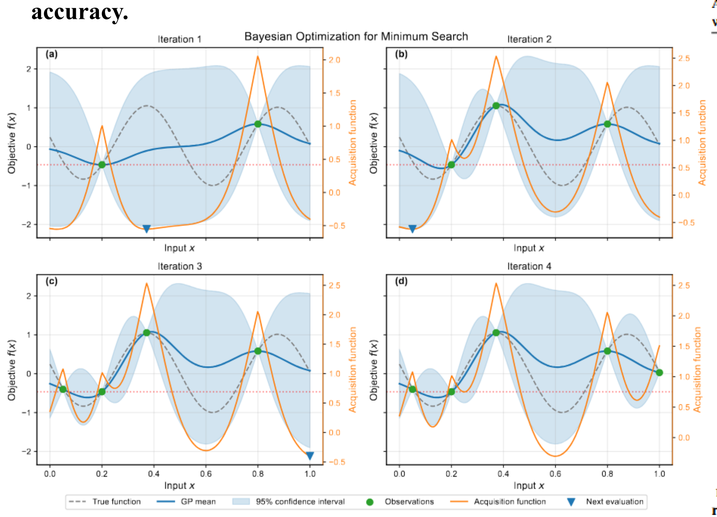

Algorithm 1 Two-step modeling method for the transformer winding.

Input: Objectives $f_{obj} = (Ob_1(x), Ob_2(x), Ob_3(x))$; initial evaluation budget $m \geq 2$; total evaluation budget $T > m$; data storage set H; initial observation set $x_{1:m}$, and evaluations $y_{1:m}$ (optional). // x and y are vector values that contain multiple parameters (i.e., values of circuit parameters) and objectives, respectively.

Output: Based on evaluations, manually choose the best observation x_{best}, y_{best} in the Pareto-optimal set. If the model-based FRA data are not very matched, constrain the search space to ±5% around x_{best} and iterate steps 3-10.

1: A transformer model is constructed using ANSYS Maxwell.
2: The circuit parameters are determined using the FEM.
3: Set the calculated parameters in Step 1 within ±5% as the bounded search space X, $x \in$X.
4: If $x_{1:m}$, $y_{1:m}$ is not provided, let x_t be a Sobol sequence and let $y_t = f_{obj}(x_t)$, $x_t \in$ X, for $t = 1,\ldots,m$. // Construct the initial observation set and get evaluations.
5: **For** $t = m+1,\ldots,T$ **do**
6: Let $H_t = \{x_{1:t-1}, y_{1:t-1}\}$.
7: Use H_t to fit SAAS GP.
8: Use QNEHVI to obtain the next observation x_t.
9: Evaluate $y_t = f_{obj}(x_t)$. // Input the observation into the built model to obtain an evaluation.
10: **end**
return Pareto-optimal set $\{x_{1:a}, y_{1:a}\}$.

Figure 2: Illustration of the Bayesian optimization process to find the minimum of a simple function. A Gaussian process model predicts the function values (solid blue line) along with associated uncertainties (blue shading) based on previously collected data. Subsequently, an acquisition function leverages this model to evaluate the potential "value" of future measurements, thereby balancing exploration and exploitation. The next observation is then selected by minimizing the acquisition function in the parameter space. This iterative process continues until the optimization objectives are achieved.

Two-step Modeling Approach

Step 1 – FEM-based Parameter Extraction

1. A 3D transformer model is built in ANSYS Maxwell, considering physical structure and insulation materials.
2. Finite Element Method (FEM) is used to calculate inductance, capacitance, and resistance parameters.

Step 2 – Circuit Simulation + Bayesian Optimization

1. An equivalent circuit is implemented in Simulink.
2. Parameter search space is defined as ±5% around FEM-derived values.
3. Multi-objective Bayesian Optimization (MOBO) is applied with three objectives:
   - Ob1: overall fitting accuracy $Ob_1 = \sum_{i=1}^{N}\left(\frac{T_{actual}(w_i) - T_{model}(w_i)}{T_{actual}(w_i)}\right)^2$
   - Ob2: similarity between measured and simulated FRA data $Ob_2 = \sum_{i=1}^{N}\left(\frac{T_{actual}(w_i) - T_{model}(w_i)}{T_{actual}(w_i)}\right)^2 + \beta\left(\frac{\sum_{i=1}^{N}(T^*_{actual}(w_i)T^*_{model}(w_i))}{\sqrt{\sum_{w=1}^{N}(T^*_{model}(w_i))^2\sum_{w=1}^{N}(T^*_{actual}(w_i))^2}}+1\right)^{-1}$
   - Ob3: resonance point fitting accuracy $Ob_3 = \sum_{i_{RP}=1}^{N_{RP}}\left(\frac{T_{actual}(w_{i_{RP}}) - T_{model}(w_{i_{RP}})}{T_{actual}(w_{i_{RP}})}\right)^2$ $T^*(w_i) = |T(w_i)| - \frac{1}{N}\sum_{i=1}^{N}|T(w_i)|$
4. SAAS Gaussian Process and qNEHVI acquisition function are used for efficient high-dimensional optimization.

Experiment results

Experimental subject and setup

- A specially designed 10 kV transformer was used, built according to conventional 110 kV design principles.
- High-voltage winding: 30-disk disc-type structure (interleaved + double-disk continuous).
- Low-voltage winding: 6-layer layer-type structure.
- Focus: A-phase high-voltage winding, modeled with 30 equivalent units.

Figure 3: Internal structure of the specially designed 10 kV transformer.

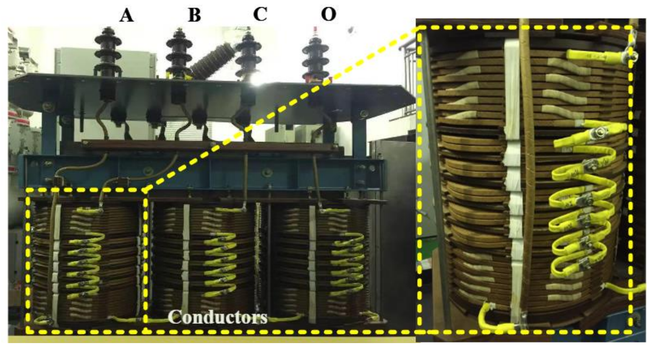

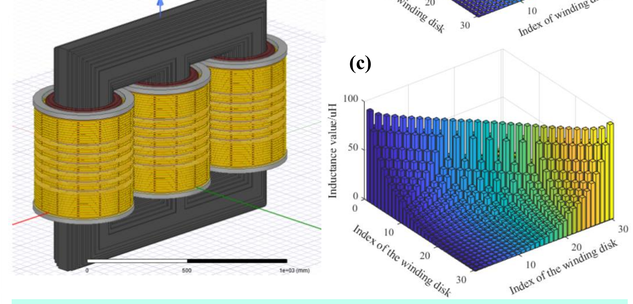

Figure 4: FEM-based model and results. (a). 3D finite element model of transformer. (b). Capacitance value between different disks. (c). Self-inductance and mutual inductance of different disks.

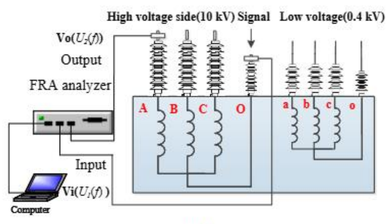

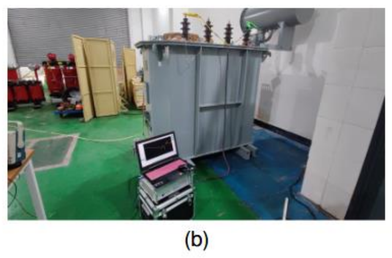

Figure 5: Measurement experimental diagram. (a) Measurement wiring diagram. (b) Actual wiring diagram.0 200

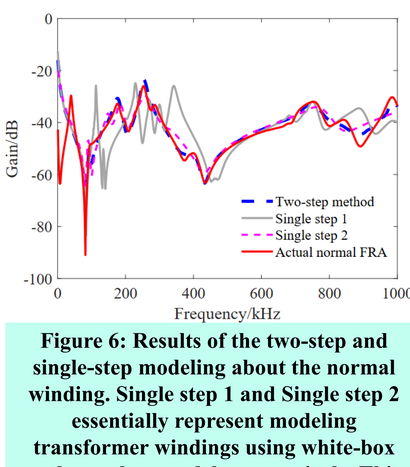

Figure 6: Results of the two-step and single-step modeling about the normal winding. Single step 1 and Single step 2 essentially represent modeling transformer windings using white-box and gray-box models, respectively. This study focuses on model-based winding fault simulation. Black-box models are excluded from consideration due to their inherent inability to simulate winding faults.

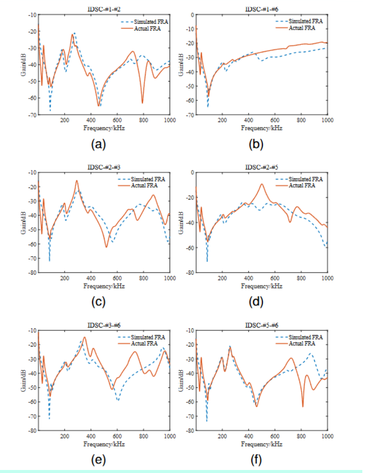

Figure 8: Several FRA data of IDSCs obtained from actual measurement and model-based simulation. (a). IDSC-#1-#2. (b) IDSC-#1-#6. (c). IDSC-#2-#3. (d). IDSC-#2-#5. (e). IDSC-#3-#6. (f). IDSC-#5-#6.

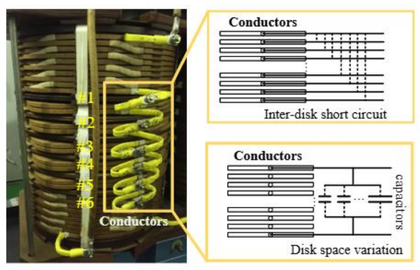

Figure 7: Simulation wiring diagram for DSVs and IDSCs. Regarding IDSCs, experimental validation can be performed by directly short-circuiting the conductors. DSVs are characterized by a reduction in the inter-disk spacing, which predominantly manifests as an increase in inter-disk capacitance within the equivalent circuit model.

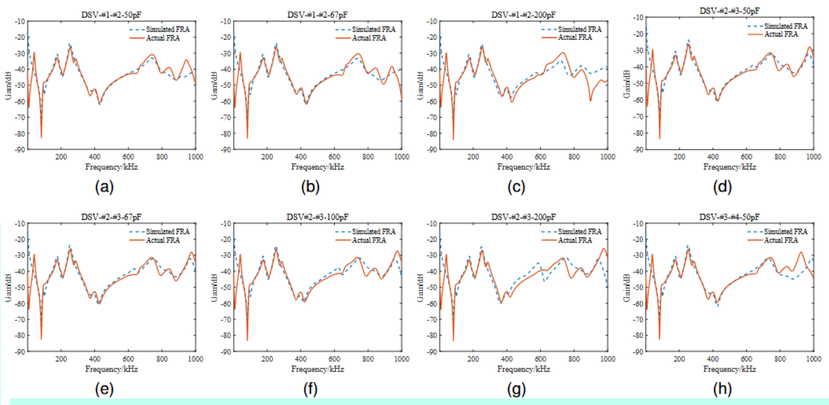

Figure 9: Several FRA data of DSVs obtained from actual measurement and model-based simulation. (a). DSV-#1-#2-50pF. (b). DSV-#1-#2-67pF. (c). DSV-#1-#2-200pF. (d). DSV-#2-#3-50pF. (e). DSV-#2-#3-67pF. (f).DSV-#2-#3-100pF. (g). DSV-#2-#3-200pF. (h). DSV-#3-#4-50pF.

Model validation

- The equivalent circuit model was tuned using Bayesian optimization.
- Simulated FRA fingerprints matched closely with measured data across the 1–1000 kHz range.
- Two fault scenarios were tested: Inter-disk short circuits (IDSCs) and Disk space variations (DSVs)
- Both simulated faults reproduced the experimental FRA shifts, confirming model accuracy.

Conclusion

- The proposed model, which employs distinct parameter values for each unit and incorporates long-distance mutual inductance and capacitance, demonstrates superior agreement with measured FRA data from a physical transformer.
- To address the challenges associated with high-dimensional parameter identification, this study employs FEM to derive an initial parameter set in Step 1. This precalculation significantly reduces the computational time required for subsequent fine-tuning of circuit parameters using optimization algorithms based on measured FRA data in Step 2. Furthermore, this method facilitates data interaction between the measured data and the built model, improving the possibility of searching for a set of feasible solutions.
- To validate the model's performance, several common winding mechanical faults are simulated. The simulated FRA changing trends exhibit strong agreement with the measured data, thereby indirectly confirming a robust mapping relationship between the model and the actual transformer. Furthermore, simulated FRA data can serve as a valuable reference for subsequent fault diagnosis.

Reference

[1] Y. Chen, et al., "Application of generative AI-based data augmentation technique in transformer winding deformation fault diagnosis," Engineering Failure Analysis, vol. 159, p. 108115, 2024.
[2] M. H. Samimi et al., "FRA interpretation using numerical indices: State-of-the-art," International Journal of Electrical Power & Energy Systems, vol. 89, pp. 115–125, 2017.
[3] C. Gezegin, et al, "A Monitoring Method for Average Winding and Hot-Spot Temperatures of Single-Phase, Oil-Immersed Transformers," IEEE Transactions on Power Delivery, vol. 36, no. 5, pp. 3196–3203, 2021.
[4] W. C. Sant'Ana et al.,, "A survey on statistical indexes applied on frequency response analysis of electric machinery and a trend based approach for more reliable results," Electric Power Systems Research, vol. 137, pp. 26–33, 2016.

✓ **ACKNOWLEDGMENTS**

This work was supported in part by the China Southern Power Grid under Grant No. ZBKJXM20232293, in part by the Fundamental Research Funds for the Central Universities under Grant SWU-KT22027, and in part by the National Natural Science Foundation of China under Grant 51807166